Carbohydrate Polymers 90 (2012) 516–523

Contents lists available at SciVerse ScienceDirect

Carbohydrate Polymers

journal homepage: www.elsevier.com/locate/carbpol

Enhancement of amygdalin activated with β-D-glucosidase on HepG2 cells proliferation and apoptosis

Cunshan Zhou[a,b,c,d,e,*], Lichun Qian[b,**], Haile Ma[a,d,e], Xiaojie Yu[a,c,d,e], Youzuo Zhang[c], Wenjuan Qu[a,d,e], Xiaoxu Zhang[b], Wei Xia[b]

[a] School of Food and Biological Engineering, Jiangsu University, 301 Xuefu Road, Zhenjiang 212013, China
[b] College of Animal Science, Zhejiang University, 866 Yuhangtang Road, Hangzhou 310058, China
[c] School of Agriculture and Food Science, Zhejiang A & F University, 88 Huancheng Road (N), Lin'an 311300, China
[d] Jiangsu Provincial Research Center of Bio-process and Separation Engineering of Agri-products, Jiangsu University, 301 Xuefu Road, Zhenjiang 212013, China
[e] Key Laboratory for Physical Processing of Agricultural Products, Jiangsu University, 301 Xuefu Road, Zhenjiang 212013, China

ARTICLE INFO

Article history:
Received 1 May 2012
Received in revised form 16 May 2012
Accepted 19 May 2012
Available online 28 May 2012

Keywords:
Amygdalin
β-D-Glucosidase
HepG2 cells
Proliferation
Apoptosis

ABSTRACT

The growth inhibition and induction of apoptosis brought by amygdalin and activated with β-D-glucosidase were tested for cytoactivity in HepG2 cells. The MTT viability assay showed that all samples had effects on HepG2 proliferation in dose and time response manners. IC_{50} of stand-alone amygdalin and activation with β-D-glucosidase on the proliferation of HepG2 cells for 48 h were 458.10 mg/mL and 3.2 mg/mL, respectively. Moreover, apoptotic cells were determined by AO/EB (acridine orange/ethidium bromide) fluorescent staining method and Annexin V-FITC/PI staining flow cytometry cell cycle analysis. With increasing of amygdalin concentration and the incubation time, the apoptotic rate was heightened. Compared with the control, there was significant difference ($p < 0.01$). Together, these findings indicate that amygdalin had no strong anti-HepG2 activity; however the ingredients of amygdalin activated with β-D-glucosidase had a higher and efficient anti-HepG2 activity. It was therefore suggested that this combination strategy may be applicable for treating tumors with a higher activity.

1. Introduction

Amygdalin (D-mandelonitrile-β-D-gentiobioside, Fig. 1A), $C_{20}H_{27}NO_{11}$, is a cyanogenic glucoside initially isolated from the seeds of bitter almonds (*Prunus dulcis*) and other food plants such as linseed and manioc (Chwalek & Plé, 2004). Amygdalin is sometimes confused with laevomandelonitrile (Cyanophenylmethyl -β-D-glucopyranosiduronic acid, Fig. 1B), $C_{14}H_{15}NO_7$, which is commonly known as laetrile. However, amygdalin and laetrile are different chemical compounds (Andrew, Roscoe, & Andrew, 1980; Du et al., 2005). The amygdalin compound is known to change to its epimer, neoamygdalin (L-mandelonitrile-β-D-gentiobioside) (Fig. 1A) in water (Koo et al., 2005). It is a controversial anti-tumor natural product that has been used as an alternative cancer drug for many years. Since the early 1950s, a modified form of amygdalin has been developed under the names "laetrile" and "Vitamin B_{17}" to cure cancer, but it is not a Vitamin. Studies have found it to be ineffective, dangerously cause cyanide posisoning, and sometimes fatal under realistic conditions (Fig. 1C and D). It is also decomposed by the action of β-D-glucosidase to yield hydrocyanic acid which stimulates the respiratory center reflexively and produces a kind of antitussive and antiasthmatic effects (Badr & Tawfik, 2010; Lv, Yu, & Zheng, 2005).

Previous studies on amygdalin have focused on its purification, toxicity related to the release of cyanide, anti-tumor mechanism, and identification of its metabolites in plasma or herbs, and its pharmacological effect on cancers (Rauws, Gramberg, & Olling, 1982). Besides the antitumor activity, amygdalin has also been used for the treatment of asthma, bronchitis, emphysema, leprosy and diabetes.

Amygdalin has been used as a traditional drug because of its wide range of medicinal benefits, including curing or preventing cancer, relieving fever, suppressing cough, and quenching thirst. In the late 1970s and early 1980s, amygdalin was reported to selectively kill cancer cells at the tumor site without systemic toxicity and to effectively relieve pain in cancer patients. However, the Food and Drug Administration (FDA) has not approved amygdalin as a cancer treatment owing to insufficient clinical evidence of its efficacy and potential toxicity. Despite the failure of clinical tests to demonstrate the anticancer effects of amygdalin in the U.S.A. and

* Corresponding author at: School of Food and Biological Engineering, Jiangsu University, 301 Xuefu Road, Zhenjiang 212013, China. Tel.: +86 511 88790958; fax: +86 511 88790958.
** Corresponding author at: School of Food and Biological Engineering, Jiangsu University, 301 Xuefu Road, Zhenjiang 212013, China. Tel.: +86 571 86994963; fax: +86 571 86994963.
E-mail addresses: cunshanzhou@163.com (C. Zhou), lcqian@zju.edu.cn (L. Qian).

0144-8617/$ – see front matter © 2012 Elsevier Ltd. All rights reserved.
http://dx.doi.org/10.1016/j.carbpol.2012.05.073

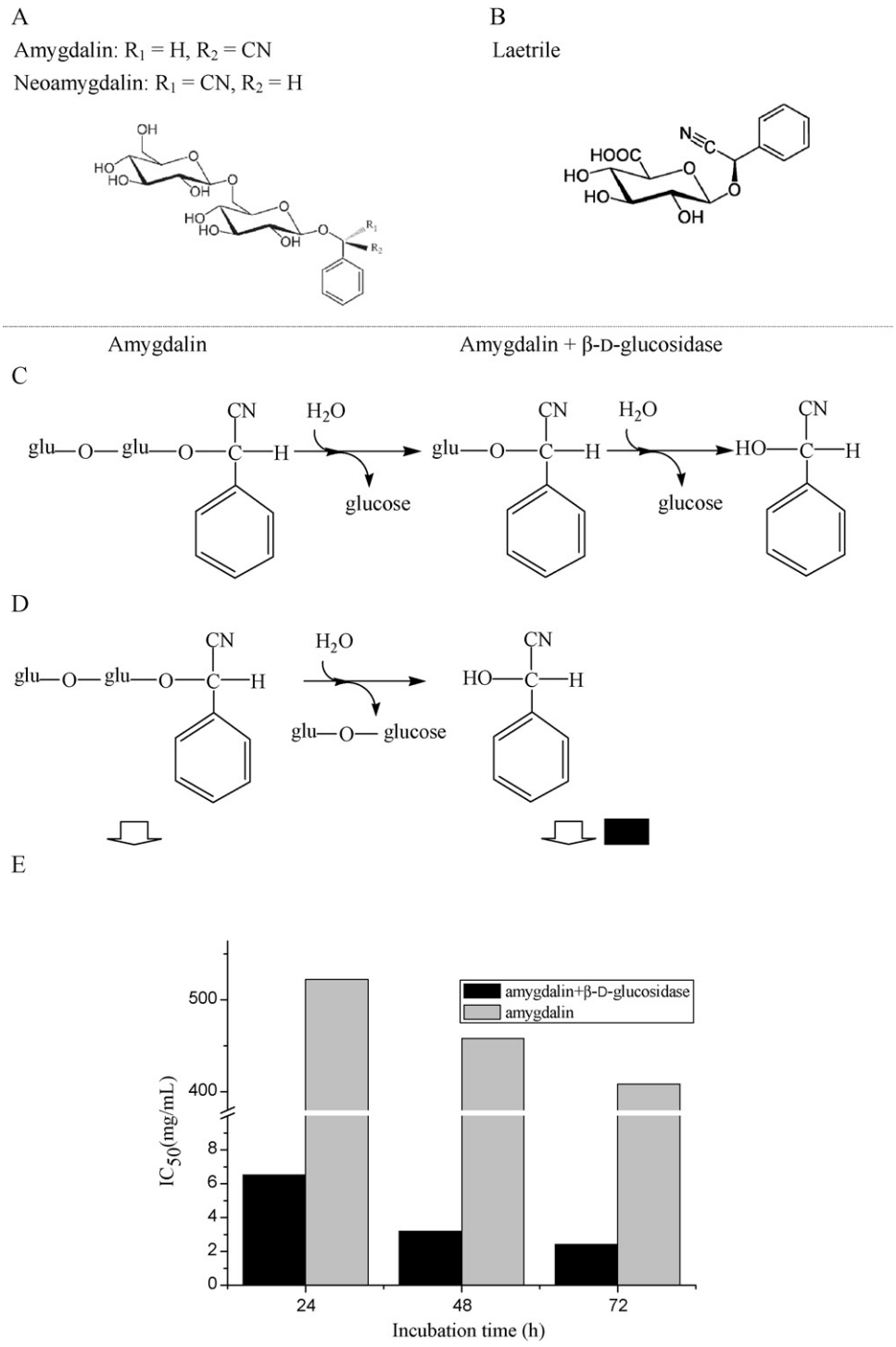

Fig. 1. (A–E) Molecular structure of amygdalin, laetrile and hydrolysis process of amygdalin, IC_{50} of amygdalin itself and activated with β-D-glucosidase. (A) Molecular structure of amygdalin (D-mandelonitrile-β-D-gentiobioside, $C_{20}H_{27}NO_{11}$). (B) Molecular structure of laetrile (cyanophenylmethyl-β-D-glucopyranosiduronic acid, $C_{14}H_{15}NO_7$). (C) Hydrolysis of amygdalin by a typical sequential mechanism of two step hydrolytic reactions. (D) Hydrolysis of amygdalin by a simultaneous mechanism of one step hydrolytic reactions. (E) IC_{50} of amygdalin itself and activated with β-D-glucosidase on the proliferation of HepG2 cells with different test groups for 24, 48, and 72 h. The median effective dose (IC_{50}), which is the amount of samples able to inhibit cell proliferation by 50%, was calculated graphically for each cell proliferation curve (a plot of inhibition of cell proliferation (%) *versus* concentration (graph not shown) which yielded a linear equation, part values are shown in).

in Europe, amygdalin continues to be manufactured and administered as an anticancer therapy in northern Europe and Mexico (Chang, Shin, & Yang, 2006; Kwon, Lee, & Hong, 2010). Few studies have investigated its pharmacological effects on HepG2 cells.

Recently, studies by Chang and Zhang (2012) demonstrated that amygdalin itself has no anti-tumor activity *in vitro*, but rather the active ingredients were determined to be amygdalin degradation products. However, amygdalin has been recognized having anti-tumor activity *in vivo* for a long time. Further studies on this subject are rather limited.

It is known that, in the intestine, the enzyme complex emulsin containing the enzymes β-D-glucosidase, benzocyanase, and others, may degrade the amygdalin into many components. The growth inhibition and the induction of apoptosis brought by

amygdalin itself and activation with β-D-glucosidase were tested for cytoactivity in the human hepatocellular carcinoma cell line HepG2. Therefore, the objectives of the current study were: (a) to examine the effects of amygdalin on human HepG2 cells and to characterize the apoptosis involved; (b) to investigate the effect of amygdalin activated with β-glucosidase on HepG2 cells proliferation and apoptosis.

2. Materials and methods

2.1. Materials

Cell culture medium and reagents were purchased from Gibco Laboratories (Grand Island, NY, USA). HepG2 (HB 8065) cell line was obtained from the Type Culture Collection of the Chinese Academy of Science Cell Bank and preserved in our laboratory. Amygdalin, streptomycin, penicillin, L-glutamine and dimethyl sulfoxide (DMSO) were all greater than 98% in purity (Sigma–Aldrich Corp.). All other chemicals made in China were of analytical grade. Culture media and antibiotics were purchased from Gibco (Grand Island, NY, USA), 0.25% trypsin–EDTA, fetal bovine serum (FBS), β-D-glucosidase (37 U/mg), and nonessential amino acids (NEAA) were obtained from Sigma–Aldrich (Steinheim, Germany). The 3-(4,5-dimethylthiazo-2-yl)-2,5-diphenyl-tetrazolium bromide (MTT) kit, the acridine orange/ethidium bromide (AO/EB) fluorescent staining kit, and Annexin V-FITC/PI apoptosis detection kit (KeyGEN Biotech, Nanjing, China).

2.2. Cell culture

The human hepatoma HepG2 cells (a human hepatoblastoma cell line with a wide variety of liver-specific metabolic responses to different kinds of drugs) (Knowles, Howe, & Aden, 1980) were routinely cultured in RPMI1640 medium supplemented with 10% (v/v) heat-inactivated fetal bovine serum (FBS), 100 U/mL penicillin, 100 μg/mL streptomycin, 1% non-essential aminoacids and 2 mmol/L L-glutamine, in a humidified atmosphere of 95% air–5% CO_2 at 37 °C. The cells were subcultured every 7 days at 1:3 split ratios. The cells were used for experiments within eight passages to ensure cell line stability. The medium was changed every 2 days whiles the stocked cells were routinely frozen and stored in liquid N_2.

Stock solutions of amygdalin (140 mg/mL) and β-D-glucosidase (1 mg/mL) were freshly prepared in serum-free RPMI1640 and then filtered through 0.22 μm sterile cellulose acetate syringe filters. The control cells received an equivalent amount of RPMI1640.

2.3. Cell proliferative MTT assay dose–response

The MTT assay was used to evaluate the antiproliferative activities of amygdalin and the degradation group tests. The assay is based on the cleavage of the yellow tetrazolium salt MTT into purple formazan by metabolically active cells, which can be photometrically quantified (Mosmann, 1983). An increase in the number of living cells results in an increase in total metabolic activity, which leads to a stronger color formation.

For the assays, cells (5×10^3 cells/well in 180 μL of complete RPMI1640) were placed in each well of a 96 well flat bottom plate. The cells were allowed to adhere for 24 h, and then 20 μL of the complete cell growth medium of different concentrations of samples were added to the cells. The blank wells contained the above concentrations of samples in 200 μL of growth medium but with no cells. After 24, 48, 72 and 96 h of incubation, the media were replaced with 200 μL of serum-free RPMI1640. To each well was added 50 μL of MTT solution (5 mg/mL). After 4 h of postincubation, the medium was removed and 100 μL of DMSO was added to each well in order to solubilize the formazan. The plate was read using a Labsystem multiskan MCC/340 microplate reader (Thermo Electron Corporation, Barcelona) at a wavelength of 570 nm with a reference wavelength of 690 nm. The results are expressed as the percentage of viable cells with respect to the control.

$$\text{Inhibitory of cell proliferation (\%)} = \left[\frac{\text{Mean absorbance of the control} - \text{Mean absorbance of the sample}}{\text{Mean absorbance of the control}}\right] \times 100$$

The median effective dose (IC_{50}), which is the amount of samples able to inhibit cell proliferation by 50%, was calculated graphically for each cell proliferation curve.

2.4. Cell morphology and adhesion

Cells were seeded on 35 mm Petri dish at a density of 1×10^5 cells/mL with or without indicated concentrations of the samples and the test groups. At each of the incubation periods (24 h, 48 h, 72 h), the cells were observed under a microscope (TE2000-U, Nikon Corporation).

2.5. Apoptosis induction with AO/EB double staining assay

The cells seeded and treated with the test groups at the various concentrations were dyed *in situ* with 2 μL mixture of 100 mg/L AO and 100 mg/L EB, and observed under a fluorescence microscope (Eclipse E 600 Nikon, Italy). Double staining allows discrimination of live (L) cells from early apoptotic (EA), late apoptotic (LA) and necrotic cells (N). The AO permeates all cells and stains the nuclei green as a result of intercalation in double-stranded DNA or orange when it binds to single stranded RNA and accumulates in lysosomes. The EB is absorbed only by cells with a damaged cytoplasmic membrane, and the nucleus of LA and N cells is stained red. EB dominates over AO. L cells have a normal green nucleus; EA cells display a bright green nucleus with condensed or fragmented chromatin; in LA cells condensed and fragmented chromatin is stained orange; finally, N cells have an orange stained, structurally normal nucleus (Giantomassi et al., 2010).

The percentage of apoptotic cells was calculated as the ratio of apoptotic cells to total cells. Morphometric analysis was performed on digital images recorded with the Coolpix camera at the same magnification in 20 randomly selected fields per treatment using the Lucia image analyzer. L, N, EA and LA cells were expressed as percent values of all cells counted (Aljandali et al., 2001; Baskić, Popović, Ristić, & Arsenijević, 2006). A minimum of 400 cells were counted for each treatment.

$$\text{The apoptosis rate (\%)} = \left[\frac{\text{Early apoptotic cells} + \text{Late apoptotic cells}}{\text{Total cells}}\right] \times 100$$

2.6. Analysis of apoptosis with Annexin V-FITC/PI staining assay

HepG2 cells (5×10^5 cells/well), grown in 6-well plates for 24 h were used for Annexin V-FITC/PI experiments. Apoptosis or necrosis was determined using an Annexin V-FITC/PI apoptosis detection kit as previously described (Dey & Cederbaum, 2006), which is based on the observation that soon after initiating apoptosis, cells translocate the membrane phosphatidylserine (PS) from the inner face of the plasma membrane to the cell surface, but they also shrink, increasing their side scatter (SS) and reducing their forward scatter (FS) characteristics. Once on the cell surface, PS can be

easily detected by staining with a fluorescent conjugate of Annexin-V, that has a high affinity for PS. Cells that have Annexin-V-FITC bound on their surface (early apoptotic) show a green membrane fluorescence, while cells that have lost membrane integrity will show an homogeneous red fluorescence (propidium iodide, PI) of the nucleus and a halo of green staining (FITC) on the cell surface (late apoptotic or necrotic cells).

In brief, untreated and treated HepG2 cells were collected, washed twice in ice-cold PBS, and then resuspended in binding buffer at a density of 5×10^5 cells/mL. Then cells were harvested and resuspended with trypsin, stained with fluorescein isothiocyanate (FITC)-labeled Annexin V (10 μg/mL) and PI (20 μg/mL) at 37 °C for 15 min in the dark and analyzed by flow cytometry using excitation/emission wavelengths of 488/525 nm and 488/675 nm for Annexin V and PI, respectively. Apoptotic cells positively stained with Annexin V showed green fluorescence and necrotic cells appeared as red fluorescent cells.

Generally, in FACS analysis, Annexin V+/PI− were regarded as apoptosis (early apoptotic), and Annexin V+/PI+ were regarded as necrosis (late apoptotic). Percentage of apoptotic cells were measured by the fluorescence-activated cell sorter analysis in a FACS analyzer (Becton Dickinson), and was calculated as the ratio of apoptotic cells to total cells.

$$\text{The apoptosis rate (\%)} = \left[\frac{\text{Annexin V} + /\text{PI} - + \text{Annexin V} + /\text{PI}+}{\text{Total cells}}\right] \times 100$$

2.7. Statistical analysis

Data were expressed as mean ± standard deviation (SD), SPSS 14.0 statistical package (SPSS Inc., Chicago, IL, USA) was performed for determination of statistical significance. Difference between two groups was analyzed by Student's *t*-test, and difference among three or more groups was analyzed by using Duncan's multiple range tests. Difference with different letters $p < 0.01$ was considered statistically significant.

3. Results

3.1. Effects on proliferation of HepG2 cells

To investigate the effect of stand-alone amygdalin and the one activated with β-D-glucosidase on cell proliferation, MTT assays were performed with different concentrations of amygdalin. The inhibitory effects on the proliferation for HepG2 cells with test groups post treatment of different concentrations are presented in Table 1. Compared with the control, the inhibition of the HepG2 cells proliferation increased significantly ($p < 0.01$) with increasing amygdalin concentrations and incubation time in the range 0–14 mg/mL, and 24–72 h, respectively. As can be seen from Table 1, the incubation with amygdalin inhibited HepG2 cell proliferated in a dose and time-dependent manner.

The median effective dose (IC_{50}), which is the amount of samples able to inhibit cell proliferation by 50%, was calculated graphically for each cell proliferation curve. The IC_{50} of the stand-alone amygdalin and β-D-glucosidase activated one on the proliferation of HepG2 cells (Fig. 1E) for 48 h were 458.10 mg/mL and 3.2 mg/mL, respectively. The values of IC_{50} indicated in Fig. 1E show that the presence of the β-D-glucosidase hydrolysis on amygdalin resulted in a significant (almost 150-fold) increase in the growth inhibition.

3.2. Effects on morphology and adhesion of HepG2 cells

Change of the morphology of HepG2 cells with amygdalin treatment of test groups at 24 h is shown in Fig. 2. Compared with the control, the volume of the treated cells was relatively smaller and the protuberance and disfiguration appeared in the cell membrane. At 72 h, the treated cells were easy to pile up together (Fig. 2), which suggested that the treatment of test groups increased the adhesion ability of the HepG2 cells.

Table 1
Effects of amygdalin itself and activated with β-D-glucosidase on the proliferation of HepG2 cells.

Test groups	Inhibition of cell proliferation (%)		
	24 h	48 h	72 h
Amygdalin[a]			
Control	0d	0c	0e
1.75	2.10 ± 0.30c	4.03 ± 0.91b	5.43 ± 1.12d
3.50	3.57 ± 0.45bc	5.50 ± 1.32b	7.83 ± 0.47c
7	4.53 ± 0.55b	10.87 ± 1.21a	12.23 ± 0.71b
14	8.13 ± 1.60a	12.83 ± 1.26a	15.73 ± 1.42a
Amygdalin activated with β-D-glucosidase[b]			
Control	0e	0e	0e
I	25.93 ± 1.11d	30.37 ± 1.62d	36.93 ± 1.96d
II	39.60 ± 1.87c	51.03 ± 2.36c	63.47 ± 2.55c
III	60.33 ± 1.42b	80.43 ± 1.55b	84.87 ± 2.15b
IV	78.57 ± 1.32a	90.23 ± 1.76a	91.00 ± 2.51a

Data are presented as mean ± SD. $n = 6$, triplicate.
Controls contained test cells and culture medium, but no test compounds.
Values in column with different lowercase letters (a–d) are significantly different ($p < 0.01$) among different groups.
[a] Test group: amygdalin, 1.75, 3.5, 7.0, 14.0 mg/mL.
[b] Test group: amygdalin activated with β-D-glucosidase, I: 1.75 mg/mL amygdalin + 0.1 mg/mL β-D-glucosidase, II: 3.5 mg/mL amygdalin + 0.1 mg/mL β-D-glucosidase, III: 7.0 mg/mL amygdalin + 0.1 mg/mL β-D-glucosidase, IV: 14.0 mg/mL amygdalin + 0.1 mg/mL β-D-glucosidase.

3.3. Induced HepG2 cells apoptosis

To get the degree of apoptosis of the self and induced HepG2 cells, amygdalin on cells viability and apoptotic pathway were investigated. The results of the morphological alterations of HepG2 cells from amygdalin itself and activation with β-D-glucosidase treatment for 24–72 h were shown in Fig. 3. Treated cells stained with AO/EB and DAPI displayed nuclei condensation and fragmentation dose and time dependence. Typical phenotypes of apoptosis such as cytoplasm shrinkage and membrane blebbing were also observed.

3.4. Effects on the rate of apoptosis of HepG2 cells

The effects of amygdalin on the apoptotic rate of the HepG2 cells with AO/EB double staining measurement at 24, 48, and 72 h are

Table 2
The apoptosis rate on HepG2 cells of amygdalin activated with β-D-glucosidase by AO/EB double staining measurement and Annexin V-FITC/PI staining measurement.

Test groups	The apoptosis rate (%)		
	24 h	48 h	72 h
AO/EB double staining measurement			
Control	1.17 ± 1.04[d]	1.83 ± 0.29[d]	1.83 ± 0.29[d]
I	30.17 ± 1.04[c]	36.00 ± 1.00[c]	44.00 ± 1.00[c]
II	40.17 ± 0.76[b]	55.50 ± 2.17[b]	67.17 ± 1.04[b]
III	60.33 ± 1.04[a]	84.83 ± 0.76[a]	89.00 ± 1.00[a]
Annexin V-FITC/PI staining measurement			
Control	1.65 ± 0.27[d]	2.62 ± 0.46[d]	
I	23.58 ± 0.94[c]	28.11 ± 1.24[c]	
II	32.33 ± 1.89[b]	42.09 ± 2.09[b]	
III	51.84 ± 2.48[a]	81.46 ± 3.14[a]	

Data are presented as mean ± SD. $n = 6$, triplicate.
Controls contained test cells and culture medium, but no test compounds.
Values in column with different superscript lowercase letters are significantly different ($p < 0.01$) among different groups.

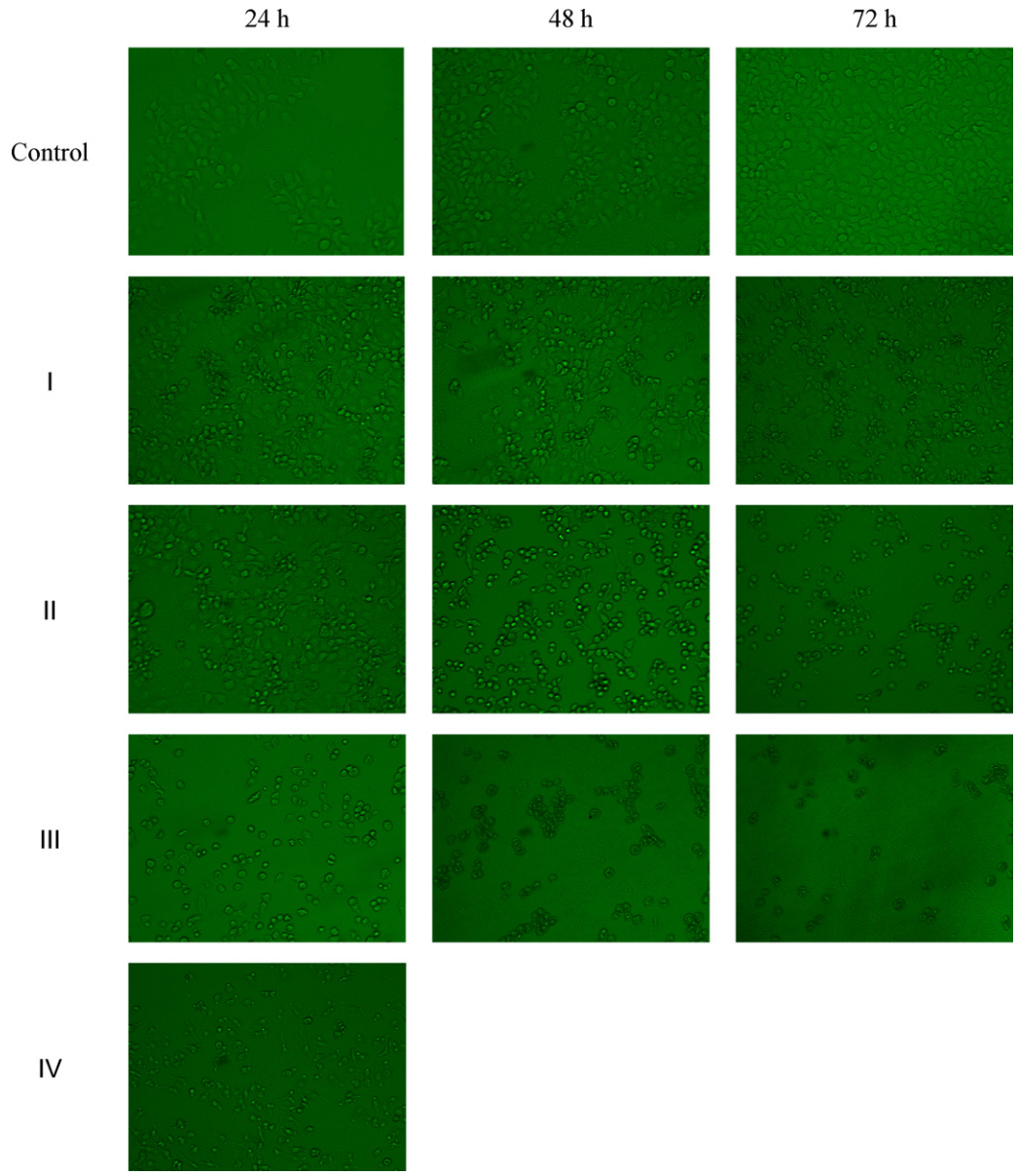

Fig. 2. Morphological changes of the cells treated with different test groups for 24, 48, and 72 h. Cells morphology was observed by a phase contrast inverted microscope (200×). Controls contained test cells and culture medium, but no test compounds.

shown in Table 2. At 24, 48, and 72 h, all test groups produced a significantly ($p < 0.01$) greater percentage of apoptosis rate compared with the control.

The effects of amygdalin on the rate of apoptosis of the HepG2 cells with flow cytometry using Annexin V-FITC/PI staining measurement at 24, 48, and 72 h are shown in Fig. 4. All treated cells displayed some morphological traits such as nuclear condensation (pyknosis) and fragmentation (karyorrhexis) consistent with the apoptotic program cell death and served as the visual confirmation of the cell cycle analysis. The apoptotic rate of the amygdalin on the HepG2 cells with Annexin V-FITC/PI staining measurement is shown in Table 2.

4. Discussion

Amygdalin has been used as a cytotoxic agent to treat cancer, though cancer patients treated with conventional therapies have used amygdalin as an alternative cancer drug for about 40 years (Nahrstedt, Sattar, & El-Zalaban, 1990). In small quantities, glycosides such as amygdalin do exhibit expectorative, sedative and digestive properties. Since its discovery in 1845, many researchers have reported the anti-tumor activity of amygdalin *in vitro*. However, some researchers reported that this "alternative cancer cure" was not supported by encouraging evidence as some of these alternative cures are associated with considerable risks (Ge, Chen, Han, & Chen, 2007). The study presented here demonstrates that amygdalin itself and activated with β-D-glucosidase, inhibit proliferation and induces apoptosis in human hepatoblastoma HepG2 cells. The similar results, Tables 1 and 2 indicate that amygdalin itself had no strong anti-HepG2 activity; however the ingredients of amygdalin activated with β-D-glucosidase had efficient anti-HepG2 activity.

For better evaluation of the apoptotic features, the AO/EB Double Staining and Annexin V-FITC/PI Apoptosis Detection kit were used in the present work (Figs. 3 and 4). Apoptosis, essential in controlling cell number in many developmental and physiological settings, has been found to be impaired in many human tumors, suggesting that disruption of apoptotic function contributes

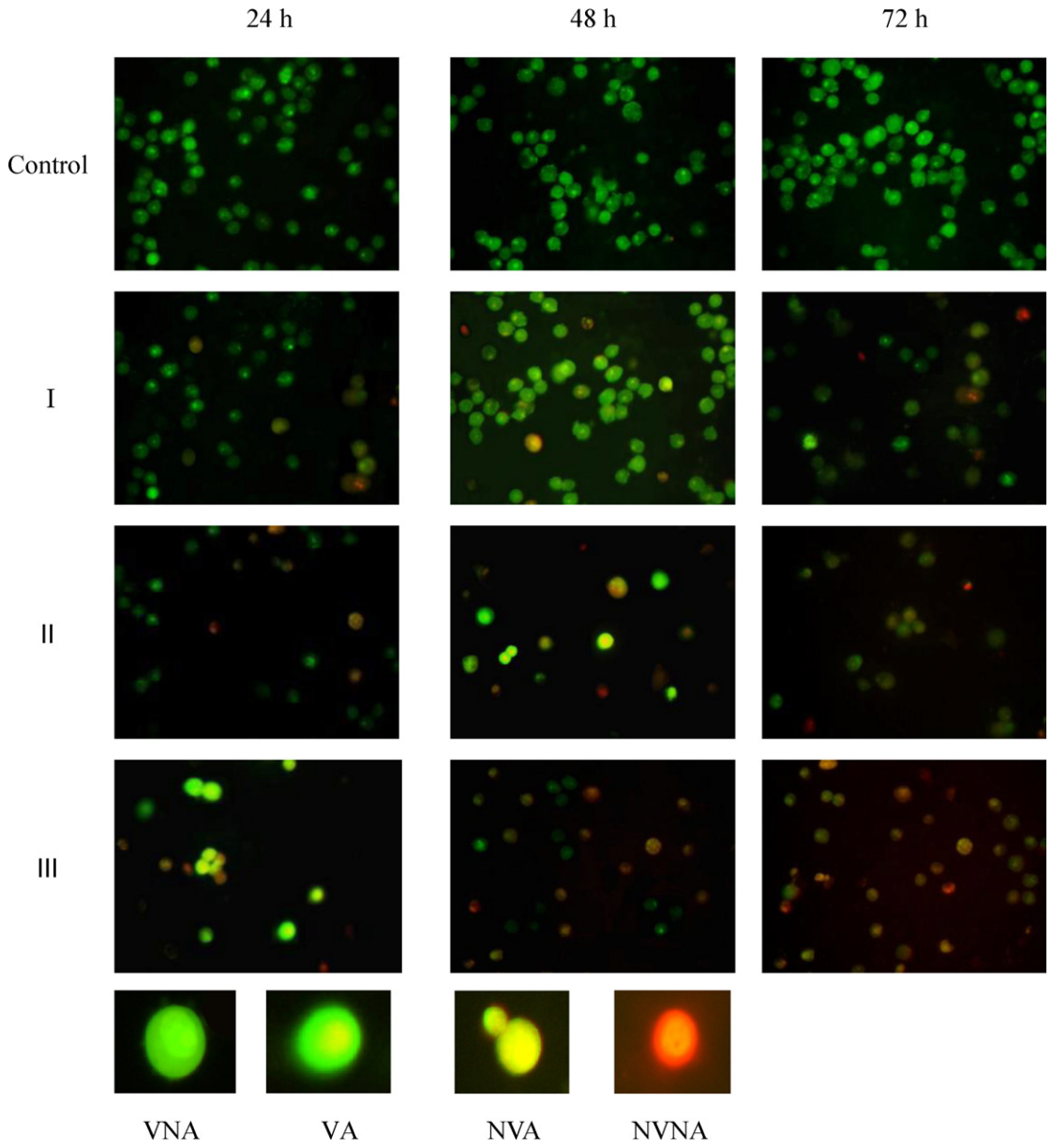

Fig. 3. Morphological changes of HepG2 cells treated with different test groups for 24, 48, and 72 h with AO/EB double staining (400×). Controls contained test cells and culture medium, but no test compounds. VNA: viable non-apoptotic cell, VA: viable apoptotic cell, NVA: non-viable apoptotic cell, NVNA: non-viablenon-apoptotic cell.

substantially to the transformation of a normal cell into a tumor cell (Kawata, Osawa, & Okabe, 2009; Lee et al., 2004; Zhang & Popovich, 2008; Zhang et al., 2011). Apoptosis is an important phenomenon in chemotherapy-induced tumor-cell killing (Lin et al., 2007; Mochizuki et al., 2009). Apoptosis was assessed by three criteria in the present work, the morphology of cells (Fig. 2), the qualitative research with AO/EB fluorescent staining method (Fig. 3) and Annexin V-FITC/PI staining flow cytometry (Fig. 4), and evaluated by the apoptosis rate (Table 2).

Amygdalin was reported to degrade into benzaldehyde, glucose and hydrocyanic acid, a key ingredient in killing tumor cells but one that is also toxic to patients (Günata, Bayonove, Tapiero, & Cordonnier, 1990; Günata, Bayonove, Cordonnier, Arnaud, & Galzy, 1990b; Nout, Tuncel, & Bimer, 1995). As shown in Fig. 1C and D, we hypothesize that the potential mechanism of degradation of amygdalin with β-D-glucosidase may occur such that amygdalin is sequentially hydrolyzed to prunasin and then mandelonitrile, a typical sequential mechanism of two step hydrolytic reactions (Fig. 1C). In addition, amygdalin is directly hydrolyzed to mandelonitrile, a simultaneous mechanism of hydrolysis of one step hydrolytic reaction (Fig. 1D). Mandelonitrile in itself may undergo spontaneous hydrolysis to hydrocyanic acid and benzaldehyde or enzymatic decomposition by benzocyanase present in the emulsin complex. Mandelonitrile glucuronide may be hydrolyzed at the tumor site by β-glucuronidase to yield hydrocyanic acid, benzaldehyde and glucuronic acid. Therefore, *in vivo* the enzyme complex emulsin containing the enzymes β-D-glucosidase, benzocyanase, and others, degrades the amygdalin into four components: hydrocyanic acid, benzaldehyde, prunasin, and mandelonitrile, which are absorbed into the lymph and portal circulations (Chang & Zhang, 2012). So, the injection for amygdalin is a better way than oral administration.

Hepatocellular carcinoma is one of the most common malignant tumors worldwide and may be one of the most common fatal cancers, especially in eastern Asian countries (Chen, Lv, Liu, & Xu, 2009; Martín et al., 2008). In cases of hepatocellular carcinoma, surgical resection is preferred. Unfortunately, many patients with this disease have metastatic disease at the time of initial diagnosis;

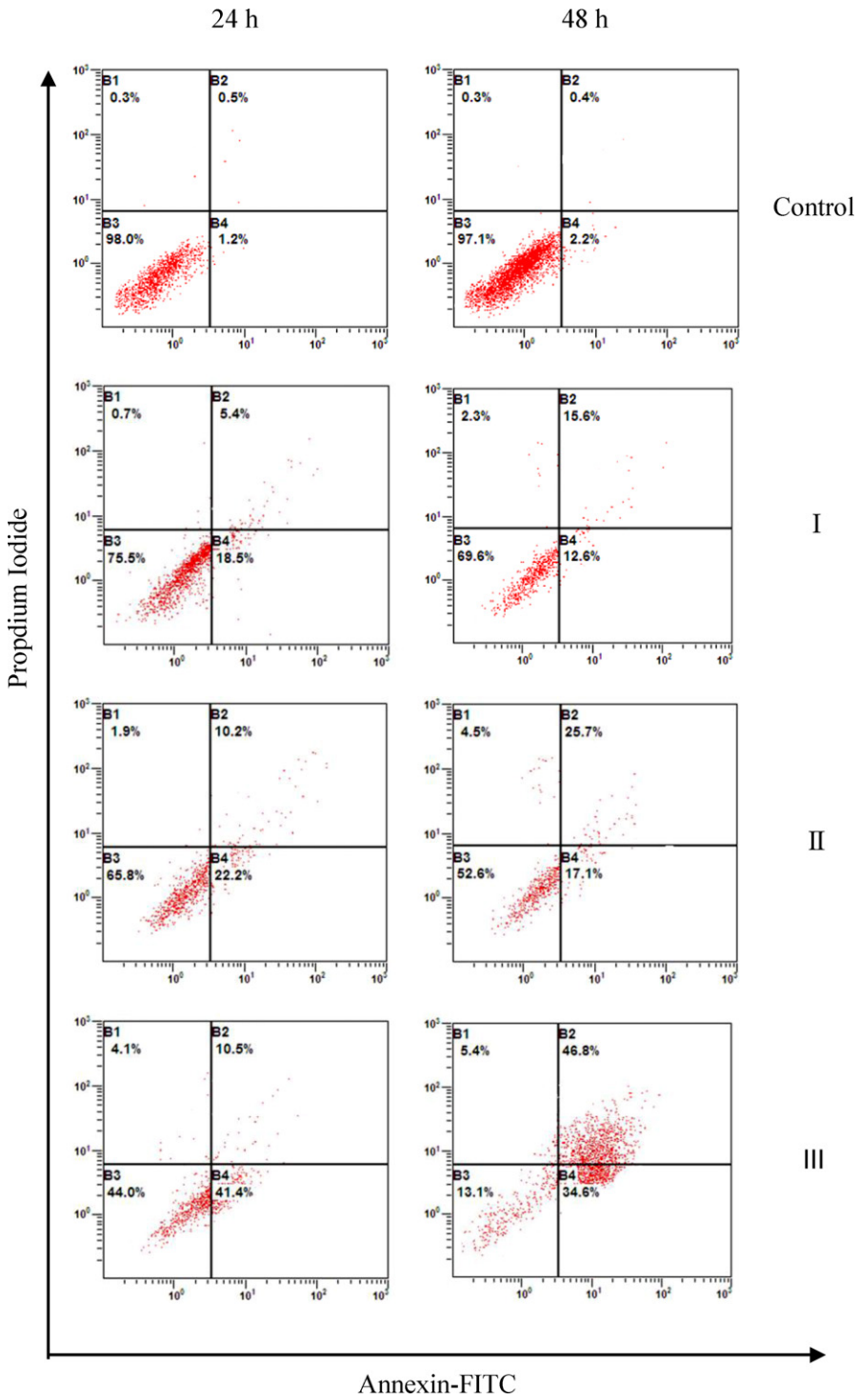

Fig. 4. Apoptosis percentage of HepG2 cells treated with different test groups for 24 and 48 h was analyzed by flow cytometry using Annexin V-FITC/PI staining. The data presented are representative of three independent experiments. Controls contained test cells and culture medium, but no test compounds.

surgical resection is usually not an ideal choice because of other pathological changes (Yoo et al., 2002). In patients with advanced disease, the average survival period is one year or less. Therefore, the development of a new therapeutic or combination strategy to this disease remains one of the most challenging areas (Colo, 1998). Based on the molecular approach, this report described a novel discovery that a treatment of amygdalin activated with β-D-glucosidase leads to an enhancement of apoptosis in human hepatoma HepG2 cells. Therapy of amygdalin activated with β-D-glucosidase may allow the use of a lower drug dose, the co-administration of these two resulted in an impressive enhancement of tumor cell killing, and it is more likely to lead to a lower toxicity and an enhancement of tumor killing. It was therefore suggested that this combination strategy may be applicable for treating tumors with a high activity. However, the actual clinical benefit for this application needs to be verified by further extensive *in vivo* testing, and without doubt, *in vivo* animal studies and human intervention studies will provide more solid evidence in this

area. Further studies are planned to determine the precise mode of cell death and cytoactive mechanism attributed to amygdalin activated with β-D-glucosidase. Studies are ongoing in our laboratory to further clarify the possible mechanisms.

5. Conclusions

In this paper, the inhibitory effects of amygdalin itself and activated with β-D-glucosidase on proliferation of cell line HepG2 were investigated. Compared with amygdalin, the activated ingredients showed stronger inhibitory effect on the proliferation rate among the cells tested. Apoptosis effects were assessed by three criteria in the work, the morphology of cell treated with the activated ingredients appeared irregular and the adhesion ability was changed among cells. Furthermore, the nuclei of the cells presented characters of apoptosis. As potential toxicity is concerned, the injection for amygdalin is a better way. Moreover, therapy of combination strategy (amygdalin activated with β-D-glucosidase) may allow with lower drug dose.

Funding sources

The work was funded by National Natural Science Foundation of China (Project nos. 31170672, 31071502, 30940058), Natural Science Foundation of Zhejiang Province of China (Project no. Y3110025), Key Laboratory of Exploitation and Preservation of Coastal Bio-resource (Project no. 2010F30003) and Key Laboratory for Physical Processing of Agricultural Products (Project no. JAPP2010-4).

References

Aljandali, A., Pollack, H., Yeldandi, A., Li, Y., Weitzman, S. A., & Kamp, D. W. (2001). Asbestos causes apoptosis in alveolar epithelial cells: Role of iron-induced free radicals. *Journal of Laboratory and Clinical Medicine*, *137*, 330–339.

Andrew, F., Roscoe, O. B., & Andrew, E. G. (1980). A β-glucosidase in feline kidney that hydrolyzes amydalin (Laetrile). *Archives of Biochemistry and Biophysics*, *201*, 363–368.

Badr, J. M., & Tawfik, M. K. (2010). Analytical and pharmacological investigation of amygdalin in *Prunus armeniaca* L. kernels. *Journal of Current Pharmaceutical Research*, *3*, 2134–2137.

Baskić, D., Popović, S., Ristić, P., & Arsenijević, N. N. (2006). Analysis of cycloheximide induced apoptosis in human leukocytes: Fluorescence microscopy using annexin V/propidium iodide versus acridin orange/ethidium bromide. *Cell Biology International*, *30*, 924–932.

Chang, H. K., Shin, M. S., & Yang, H. Y. (2006). Amygdalin induces apoptosis through regulation of bax and bcl-2 expressions in human DU145 and LNCaP prostate. Cancer cells. *Biological and Pharmaceutical Bulletin*, *29*, 1597–1602.

Chang, J., & Zhang, Y. (2012). Catalytic degradation of amygdalin by extracellular enzymes from *Aspergillus niger*. *Process Biochemistry*, *47*, 195–200.

Chen, X., Lv, P., Liu, J., & Xu, K. (2009). Apoptosis of human hepatocellular carcinoma cell (HepG2) induced by cardiotoxin III through S-phase arrest. *Experimental and Toxicologic Pathology*, *61*, 307–315.

Colo, M. (1998). The role of hepatitis C virus in hepatocellular carcinoma. *Recent Results in Cancer Research*, *154*, 337–344.

Dey, A., & Cederbaum, A. I. (2006). Geldanamycin, an inhibitor of Hsp90, potentiates cytochrome P4502E1-mediated toxicity in HepG2 cells. *Journal of Pharmacology and Experimental Therapeutics*, *317*, 1391–1399.

Du, Q., Jerz, G., He, Y., Li, L., Xu, Y., Zhang, Q., et al. (2005). Semi-industrial isolation of salicin and amygdalin from plant extracts using slow ratary counter-current chromatography. *Journal of Chromatography A*, *1074*, 43–46.

Ge, B. Y., Chen, H. X., Han, F. M., & Chen, Y. (2007). Identification of amygdalin and its major metabolites in rat urine by LC–MS/MS. *Journal of Chromatography B*, *857*, 281–286.

Giantomassi, F., Gualtieri, A. F., Santarelli, L., Tomasetti, M., Lusvardi, G., Lucarini, G., et al. (2010). Biological effects and comparative cytotoxicity of thermal transformed asbestos-containing materials in a human alveolar epithelial cell line. *Toxicology In Vitro*, *24*, 1521–1531.

Günata, Y. Z., Bayonove, C. L., Tapiero, C., & Cordonnier, R. E. (1990). Hydrolysis of grape monoterpenyl β-D-glucosides by various β-glucosidases. *Journal of Agricultural and Food Chemistry*, *38*, 1232–1236.

Günata, Y. Z., Bayonove, C. L., Cordonnier, R. E., Arnaud, A., & Galzy, P. (1990). Hydrolysis of grape monoterpenyl glycosides by *Candida molischiana* and *Candida wickerhamii* β-glucosidases. *Journal of Agricultural and Food Chemistry*, *50*, 499–506.

Kawata, K., Osawa, M., & Okabe, S. (2009). In vitro toxicity of silver nanoparticles at noncytotoxic doses to HepG2 human hepatoma cells. *Environmental Science & Technology*, *43*, 6046–6051.

Knowles, B., Howe, C., & Aden, D. (1980). Human hepatocellular carcinoma cell lines (HepG2) secrete the major plasma proteins and hepatitis B surface antigen. *Science*, *209*, 497–499.

Koo, J. Y., Hwang, E. Y., Cho, S., Lee, J. H., Lee, Y. M., & Hong, S. P. (2005). Quantitative determination of D-amygdalin epimers from armeniacae semen by liquid chromatography. *Journal of Chromatography B*, *814*, 69–73.

Kwon, H. J., Lee, J. H., & Hong, S. P. (2010). Improvement of the extraction efficiency of d-amygdalin from Armeniacae Semen powder through inactivating emulsion and suppressing the epimerization of D-amygdalin. *Archives of Pharmacal Research*, *33*, 81–86.

Lee, K. R., Kozukue, N., Han, J. S., Park, J. H., Chang, E. Y., Baek, E. J., et al. (2004). Glycoalkaloids and metabolites inhibit the growth of human colon (HT29) and liver (HepG2) cancer cells. *Journal of Agricultural and Food Chemistry*, *52*, 2832–2839.

Lin, H. M., Tseng, H. C., Wang, C. J., Chyau, C. C., Liao, K. K., Peng, P. L., et al. (2007). Induction of Autophagy and Apoptosis by the Extract of *Solanum nigrum* Linn in HepG2 Cells. *Journal of Agricultural and Food Chemistry*, *55*, 3620–3628.

Lv, W. F., Yu, D., & Zheng, R. (2005). Isolation and quantitation of amygdalin in apricot kernel and *Prunus Tomentosa* Thunb. by HPLC with solid phase extraction. *Journal of Chromatographic Science*, *43*, 383–387.

Chwalek, M., & Plé, K. (2004). Convenient syntheses of isomaltose derivatives from amygdalin. *Tetrahedron Letters*, *45*, 4749–4753.

Martín, M. A., Ramos, S., Mateos, R., Serrano, A. B. G., Izquierdo-Pulido, M., Bravo, L., et al. (2008). Protection of human HepG2 cells against oxidative stress by cocoa phenolic extract. *Journal of Agricultural and Food Chemistry*, *56*, 7765–7772.

Mochizuki, Y., Maebuchi, M., Kohno, M., Hirotsuka, M., Wadahama, H., Moriyama, T., et al. (2009). Changes in lipid metabolism by soy β-conglycinin-derived peptides in HepG2 cells. *Journal of Agricultural and Food Chemistry*, *57*, 1473–1480.

Mosmann, T. (1983). Rapid colorimetric assay for cellular growth and survival: Application to proliferation and cytotoxicity assays. *Journal of Immunological Methods*, *65*, 55–63.

Nahrstedt, A., Sattar, E. A., & El-Zalaban, S. M. H. (1990). Amygdalin acyl derivatives, cyanogenic glycosides from the seeds of *Merremia dissecta*. *Phytochemistry*, *29*, 1179–1181.

Nout, M. J. R., Tuncel, G., & Bimer, L. (1995). Microbial degradation of amygdalin of bitter apricot seeds (*Prunus armeniaca*). *International Journal of Food Microbiology*, *24*, 407–412.

Rauws, A. G., Gramberg, L. G., & Olling, M. (1982). Determination of amygdalin and its major metabolite prunasin in plasma and urine by high pressure liquid chromatography. *Pharmacy World & Science*, *6*, 172–175.

Yoo, S. M., Oh, S. H., Lee, S. J., Lee, B. W., Ko, W. G., Moon, C., et al. (2002). Inhibition of proliferation and induction of apoptosis by tetrandrine in HepG2 cells. *Journal of Ethnopharmacology*, *81*, 225–229.

Zhang, W., & Popovich, D. G. (2008). Effect of Soyasapogenol A and Soyasapogenol B concentrated extracts on Hep-G2 cell proliferation and apoptosis. *Journal of Agricultural and Food Chemistry*, *56*, 2603–2608.

Zhang, Y., Zhou, C., Tang, S., Yu, X., Kouzuma, Y., & Yonekura, M. (2011). Effect of AATI, a Bowman-Birk type inhibitor from *Apios americana*, on proliferation of cancer cell lines. *Food Chemistry*, *128*, 909–915.